

Some results of 2003 tests

1. Introduction

We present a summary of the analysis we did for selected TB'2003 runs taken in summer 2003 and imported to ITEP in July (Table 1). Our aim was to review the main features of the TB data and evaluate the observed energy resolution for electrons and pions, in the 40-200 GeV/c beam momentum range.²

Some aspects of the signal and energy reconstruction remained beyond the scope of the present analysis: a detailed signal shape study, the channel equalization, cell clusters etc. On the other hand, we made an attempt to optimize the module intercalibration for the hadronic energy reconstruction and studied the effect of the signal filtering method, as well as the event selection cuts, on the calorimeter response.

2. Signal amplitude

Let A_i be the signal value corresponding to the sample $i=0,1\dots6$. Three methods to reconstruct the signal amplitude A (to filter the signal) are considered (Fig.1):

- raw : $A=\max(A_i)$.
- parabola: A is the maximum of a parabola fit to $A_{2,3,4}$
- spline – A is the maximum the cubic spline drawn through all the samples.

A certain contribution to the energy resolution comes from the signal *quantization noise*. Its dependence on the filtering method is illustrated by a reconstruction of the simulated shaper signal³ of a random phase: the relative rms spread of the reconstructed amplitude is 6.8%, 3.7% and 2.6% for the “raw”, “parabola” and the “spline” methods, respectively. The better we approximate the signal shape, the smaller is the effect.

Similarly, the relative Gaussian σ of the electron peak in the total reconstructed energy spectrum for 4H/200 GeV/c runs (see Section 6 for details) is, respectively, 9.1% , 6.4% and 5.8%.

The spline method is used for all the numbers quoted further in this note.

3. Pedestals

We considered three methods to obtain pedestals for each cell:

<i>Table 1: Data sample used in the present analysis</i>			
beam type / position	P, GeV/c	runs #	number of events
electrons / 4H	40	2845, 2846, 2847	36000
	60	3328, 3329	24000
	100	2687, 2688	24000
	200	2967, 2968	24000
electrons / 4L	60	3242, 3243	24000
	100	2595, 2596	24000
	200	3223, 3224	24000
pions / 4H	60	3294	12000
	100	2649	12000
	200	3043	12000
pions / 4L	60	3259	12000
	100	2613	12000
	200	3193	12000

¹ With the advent of new high quality data from the September run, the results on electrons presented in this note have become somewhat obsolete. We have already circulated the summary plots and new estimates of the electron response and resolution based on new 10-100 GeV/c data. However, the analysis methods remained exactly the same. The changes compared to the original draft version of this note are mostly stylistic and aimed at better description of the methods.

² We found too few electrons in runs 3242, 3243, 3328, 3329 (60GeV/c). Therefore, the 60 GeV/c point for electrons is not presented in this note.

³ A triangular primary signal shape with $\tau=50$ ns without fluctuation of an amplitude is used.

- P1 – use \mathbf{A}_0 as a pedestal in each individual event;
- P2 – use \mathbf{A}_0 averaged over beam events in the current run;
- P3 – use pedestal events in the current run to obtain the average pedestal.

As seen from the Table 2, the method P2 gives a better energy resolution than the method P1. The methods P3 and P2 give almost identical results.

“P2 “ pedestals are further used.

4. Treatment of the “unsummed” cells

Signals from the unsummed cells are *scaled down by factor two* before adding them to integral quantities like the total response or the total noise. Thus, while a regular (“summed”) cell typically contributes an rms noise of about 3.2 ADC channels to a sum of cells, the contribution of an “unsummed” cell is about 1.6 ADC channels.

Beam	<i>P1</i>	<i>P2</i>
	$\sigma, \%$	$\sigma, \%$
E, 40GeV/c, 4H	17.2	12.9
E, 100GeV/c, 4H	14.8	11.0
E, 200GeV/c, 4H	6.4	5.8
π , 200GeV/c, 4H	14.4	11.4

5. The calorimeter response

The calorimeter response R is computed by summing all the cells together (for electrons – in FEBs 6 and 7, for pions – in FEBs 0, 1, 5, 6 and 7) or by selecting only the cells within the radius $r_{core} = 4, 8, 12, 16$ cm from the cell with the highest amplitude. We refer to these R -values as the *total* and *core* responses, respectively. For pions, we apply relative weights to FCAL2 and FCAL3:

$$R_e = \text{FCAL1 (FEB\#6,7)}$$

$$R_\pi = \text{FCAL1 (FEB\#6,7)} + g_2 \cdot \text{FCAL2 (FEB\#5)} + g_3 \cdot \text{FCAL3 (FEB\#0, 1)}$$

The intercalibration factors g_2 and g_3 are obtained by minimizing the resulting energy resolution (see Fig.3). Data favor $g_2=g_3=2$. This value is in a good agreement with $g_2=2.1$ resulting from 1998 calibrations of FCAL1 and FCAL2 with electrons.

Technically, the cell summation is performed as follows:

- first, the sample amplitudes \mathbf{A}_i in the selected cells are summed up, sample-by-sample, to obtain the sequence of 7 integrated sample amplitudes ;
- the filtering method (a spline fit in our case) is applied *to this sequence*. In the present analysis, we abandoned the alternative approach, in which the individual cell signals are first filtered and then the resulting amplitudes are summed, because of the ambiguities and fit instabilities in cells with very small or no signals.

6. Event selection

Muon counter proved to be the most effective tool to clean the data samples. Cuts on other counters and BPC's do not improve the situation (Fig.4a-4d, data - electrons, 4H, 200GeV/c), as Table 3 shows.

7. Electrons

The distributions of the calorimeter response for different core radii are shown in Fig.5. The results of the Gaussian fits of the electron peak are summarized in Table 4.

⁴ The quoted numbers correspond to the “Total response” columns of Tables 4 and 5.

Table 3: Gaussian mean total response \bar{R} and the resolution σ_R , as function of event selection cuts

Cuts#	cut description	Number of events	\bar{R} , ADC counts	σ_R , %
0.	no cuts	10561	2324	5.8
1.	PH(muon counter)<20	7872	2324	5.8
2.	Cut#1 & PH(veto counter)<10	5864	2327	5.8
3.	Cut#1 & 0.5<counters_signal<1.5 ⁵	5980	2329	5.9
4.	Cut#1 & 0.5<chambers_signal<1.5 ⁴	5791	2328	5.8
5.	Cut#1 & angleX <0.5mrad	7117	2326	5.8
6.	Cut#1 & -1mrad<angleY<-0.5mrad	7008	2329	5.8

Table 4: Gaussian mean total response \bar{R} and the resolution σ_R , as function of r_{core} cuts, for electrons

P, GeV/c	position	\bar{R} , ADC counts / σ_R , %				
		Total response	r_{core} , cm			
			4	8	12	16
40	4H	447 12.9	423 7.4	438 7.4	443 8.8	445 10.5
100	4H	1155 11.0	1096 5.5	1.131 5.3	1143 5.9	1148 7.5
	4L	1161 10.9	1107 5.4	1139 5.3	1151 5.8	1153 7.0
200	4H	2329 5.8	2237 6.4	2302 5.6	2324 5.5	2327 5.7
	4L	2196 6.4	2116 6.8	2168 6.3	2188 6.2	2193 6.2

Observations:

- 99% of R_{total} is contained in a region with $r_{core}<8\text{cm}$. The Gaussian resolution for this region can be approximated by

$$\frac{\sigma}{E} \approx \frac{160\%}{E(\text{GeV})} \oplus \frac{35\%}{\sqrt{E(\text{GeV})}} \oplus 5.2\%$$

- The resolution for R_{total} at 100 GeV/c is much too large. This results from a larger noise in runs at 100GeV/c, due to the pulser board noise. See Section 9 for more discussion.
- The R distributions are well described by Gaussian for one and half order of magnitude (Fig.6). At a lower level there is a long tail of smaller responses, which is partly due to beam pion contamination. The radial cuts reduce the tail (Fig.6-7).
- A map of energy deposited by electrons hitting the same cell in FCAL1 is shown in Fig.8. This plot represents an electromagnetic shower profile.

8. Hadrons

Distributions of R and the Gaussian fit results for pion runs are shown in Fig.8 and in Table 6.

Observations:

- The region of $r_{core}<16\text{cm}$ contains ~95% of R_{total} .
- The energy resolution plotted as function of $1/\sqrt{E}$ is shown in Fig.9. The electronic noise is subtracted. The stochastic term appears to be $\approx \frac{130 \div 140}{\sqrt{E(\text{GeV})}}\%$, the constant term – (3-5)%. The limited range of beam energies does not permit to make more precise estimates.
- Like for electrons, there is a pronounced noise problem at 100GeV/c, see Section 9.

⁵ $counters_signal = \frac{1}{3} \sum_{i=1}^3 \frac{PH(counter)_i}{median(PH_i)}$; $chambers_signal = \frac{1}{12} \sum_{i=1}^{12} \frac{PH(anode_chamber)_i}{median(PH_i)}$

Table 5: Gaussian mean total response \bar{R} and the resolution σ_R , as function of r_{core} cuts, for pions

P, GeV/c	position	\bar{R} , ADC counts / σ_R , %				
		Total response	r_{core} , cm			
			4	8	12	16
60	4H	567 28.3	337 37.5	459 24.3	512 20.7	540 20.8
	4L	589 26.4	362 30.3	468 20.0	522 17.5	548 17.4
100	4H	991 32.4	540 35.7	755 19.6	843 17.5	889 19.3
	4L	1033 33.2	593 25.0	772 16.2	865 15.3	915 18.3
200	4H	1921 11.4	1267 27.5	1654 16.6	1803 12.1	1872 10.9
	4L	1894 11.2	1305 22.8	1627 13.4	1755 10.6	1841 9.8

9. Electronic channel noise

The Table 6 shows the total rms noise in individual FEB's, evaluated by summing up all cells in pedestal events (with the “unsummed” cells scaled-down by factor 2!). Table 7 shows the noise contribution to the total response, different for electrons and pions because R_π and R_e are composed of different combinations of the FEBs. Note, that the total noise does not exactly scale up from individual FEBs, as one would expect for totally independent noise sources (this is clearly seen for FEBs 6 and 7, which are summed-up in R_e). Apparently, this is a manifestation of the coherent component of the electronic noise.

Table 6: Total rms noise of the electronic channels in individual FEBs

runs, 4H	FEB#0	FEB#1	FEB#5	FEB#6	FEB#7
e, 40GeV/c	50.9	47.8	50.8	41.5	43.1
e, 100GeV/c	57.0	66.5	63.4	65.4	60.7
e, 200GeV/c	48.3	49.2	50.8	41.2	43.4

Table 7: the contribution of the electronics noise to R_e and R_π

Runs:	e, 40, 4H	e, 100, 4H	e, 200, 4H
Total noise in contribution to R_e FEBs 6 and 7	51.8	105.0	51.9
Runs:	π , 60, 4H	π , 100, 4H	π , 200, 4H
Total noise in contribution to R_π FEBs 7,6,5,1 and 0	86.0	200.7	86.0

Observations:

- The individual channel noise for different FEB's is plotted in Fig.10. There is an additional contribution in the first thirty channels for all runs at 100 GeV/c. One can see a correlation between the FEB's (Fig.11). In 40, 60, 200GeV/c runs that kind a noise is not observed.
- This effect is associated with the pulser board that was left enabled during the physics data taking for a large fraction of 100 GeV/c runs, in order to take pulser triggers along with beam triggers. In that mode, the pulser board was demonstrated to induce a strong cross-talk to the inputs of all FEBs. The origin of the noise inside the pulser board itself remained unclear, though.
- The step-like patterns in the pedestal distributions in Fig.10 correspond to groups of “unsummed” channels, in which the signal (hence, the noise) is scaled down by two.

Figures

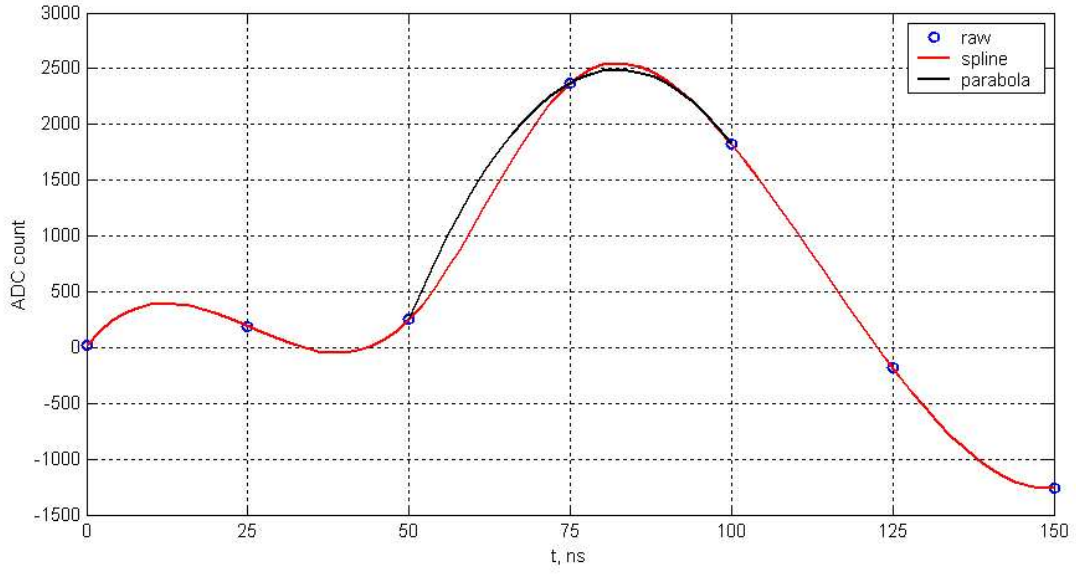


Fig.1. Example of a signal shape, electrons, 200GeV/c

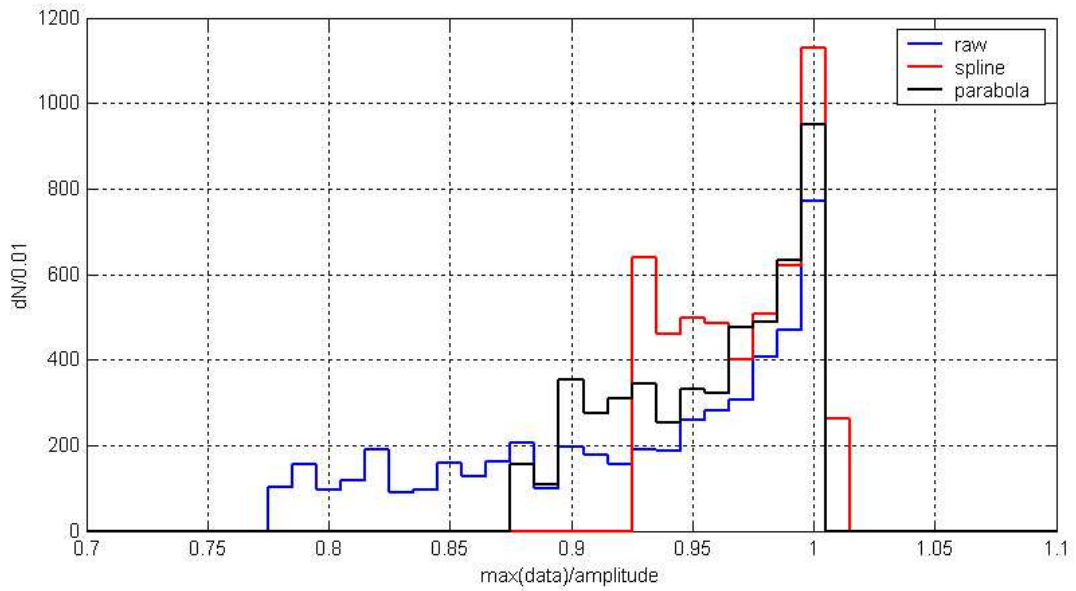


Fig.2. Reconstructed amplitude distributions, for simulated data and different filtering methods.

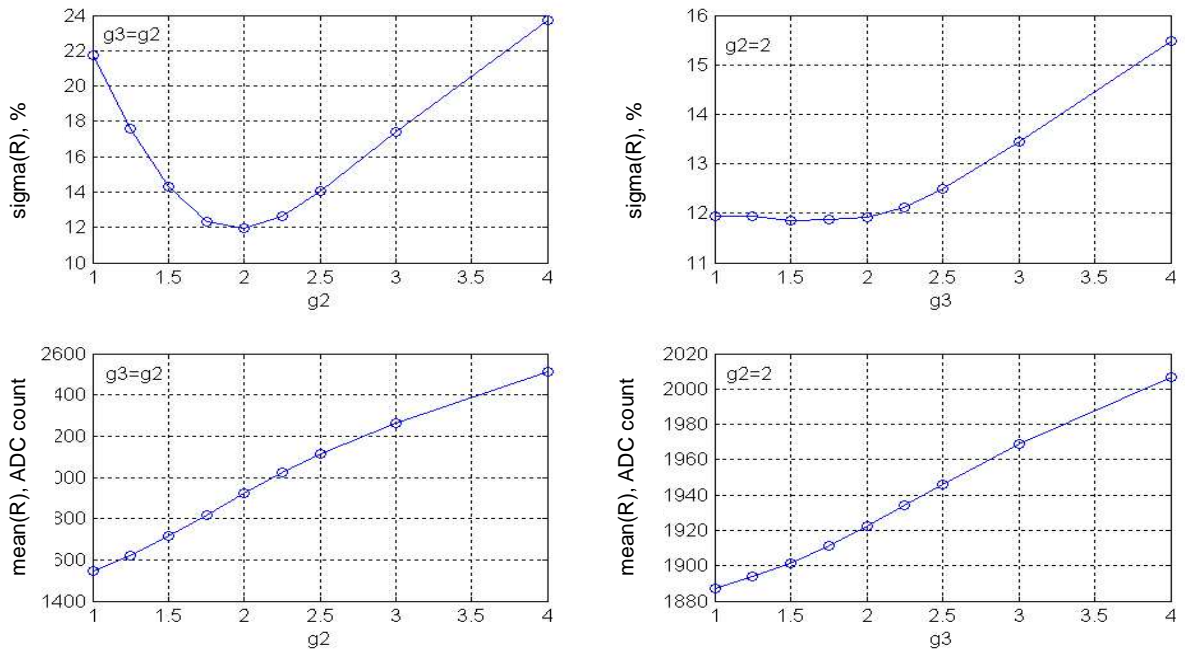


Fig.3. The effect of the intercalibration coefficients g_2 , g_3 on the response and the resolution for pions at 200GeV/c. $R = \text{FCAL1} + g_2 * \text{FCAL2} + g_3 * \text{FCAL3}$

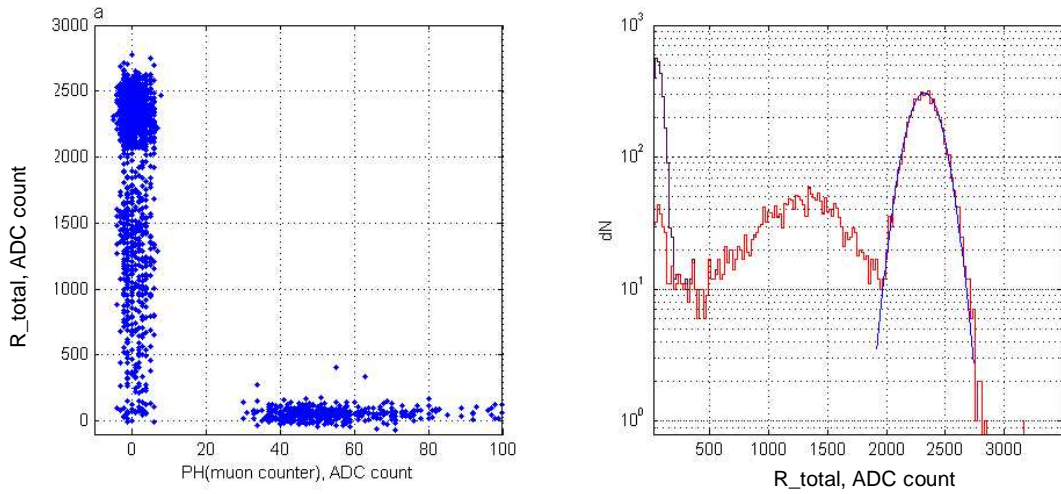


Fig.4a. Event selection, 4H, 200GeV/c,
 ___ no cuts, ___ $\text{PH}(\text{muon counter}) < 15$, ___ Gauss fit

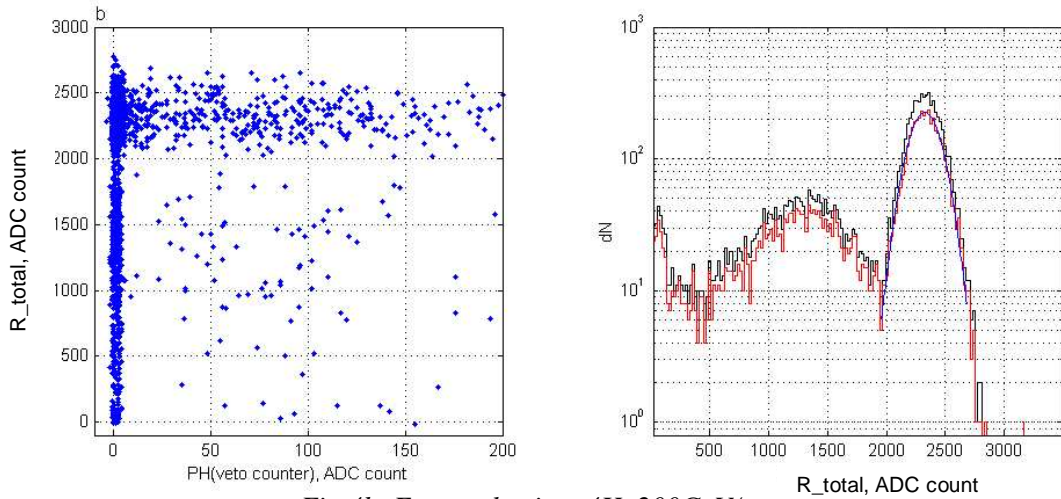


Fig.4b. Event selection, 4H, 200GeV/c,
 ___ $\text{PH}(\text{muon counter}) < 15$, ___ & $\text{PH}(\text{veto counter}) < 15$, ___ Gauss fit

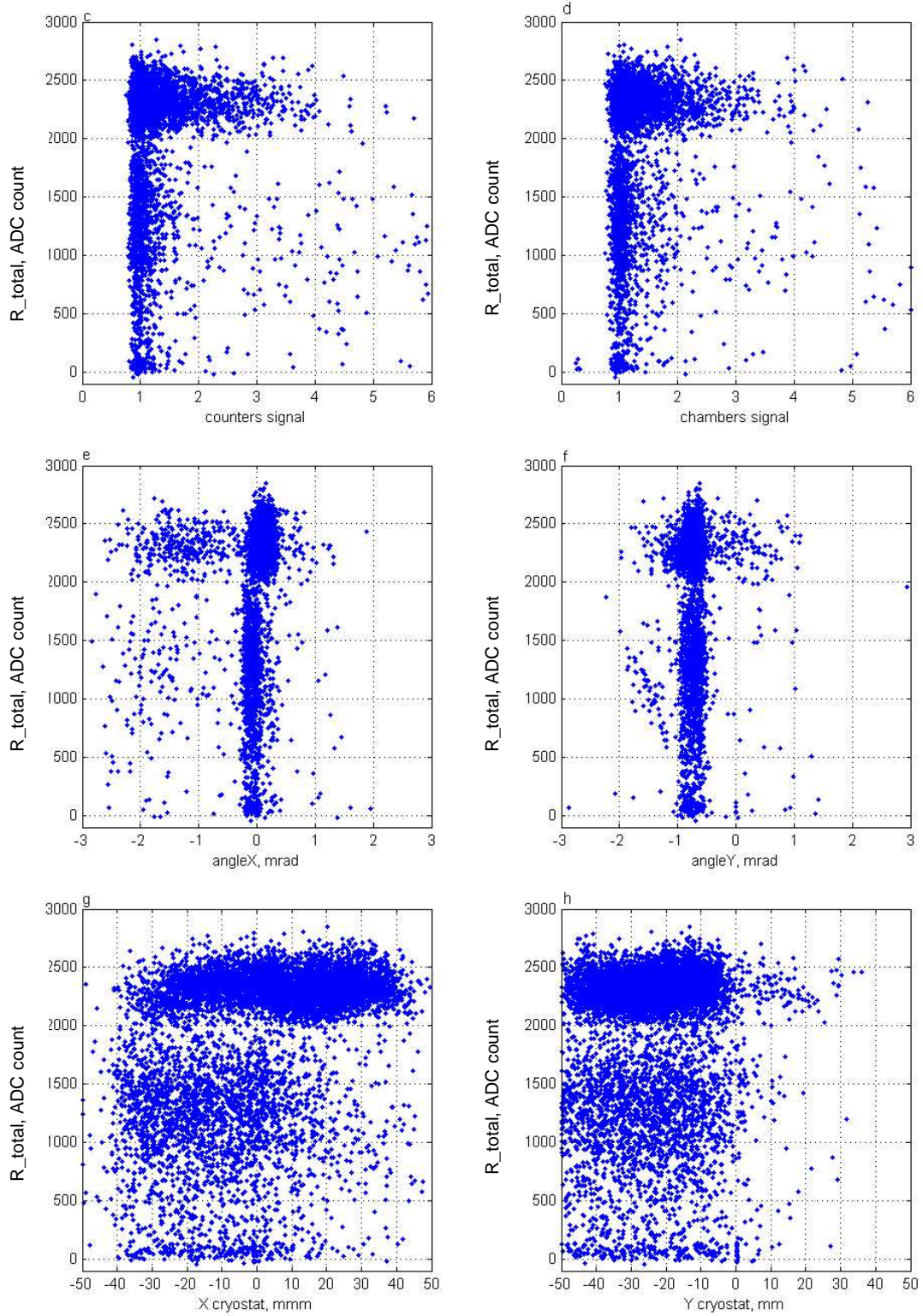
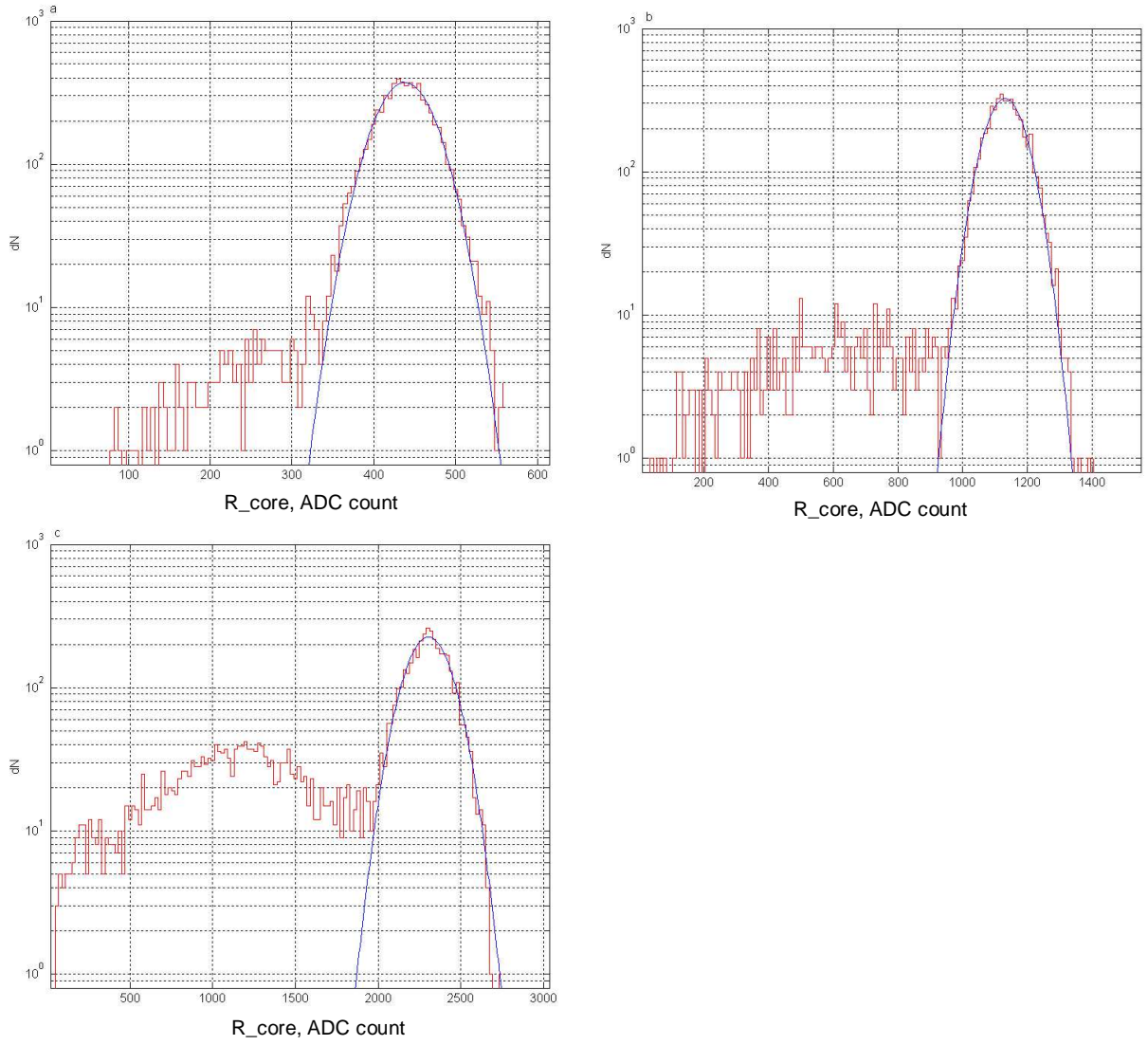


Fig.4c-h. Plots R_{total} vs.:
c – counters_signal, d – chambers_signal,
e – angleX, f – angleY,
g – X of cryostat, h – Y of cryostat.
Electrons, 4H, 200GeV/c,



*Fig.5. The distributions of $R_{core}(8cm)$, electrons, 4H:
a – $40 \text{ GeV}/c$, b – $100 \text{ GeV}/c$, c – $200 \text{ GeV}/c$*

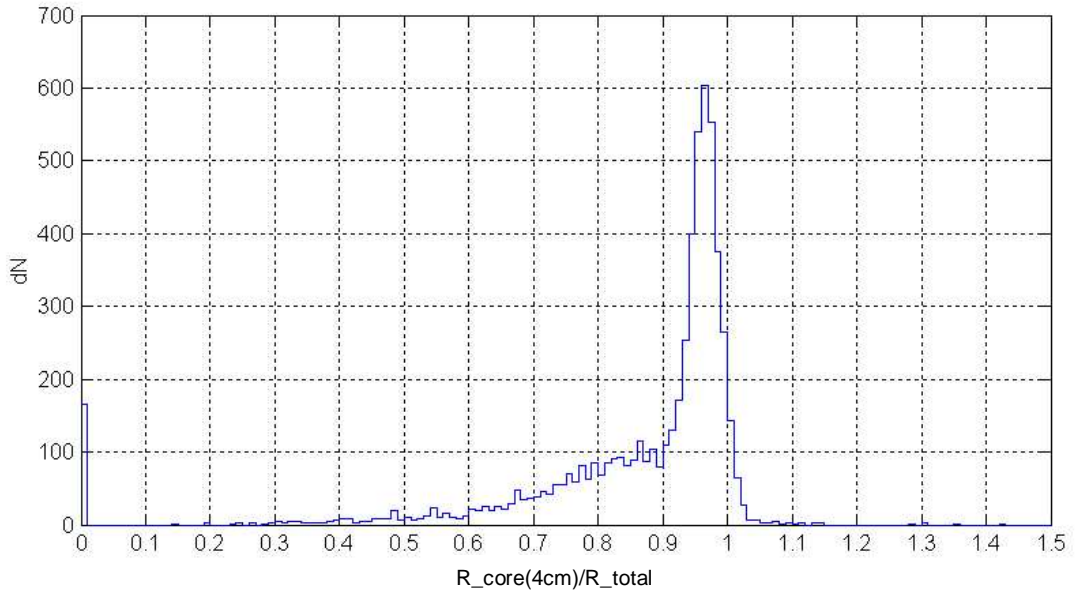


Fig.6. The distribution of $R_{core(4cm)}/R_{total}$, electrons, 4H, 200GeV/c

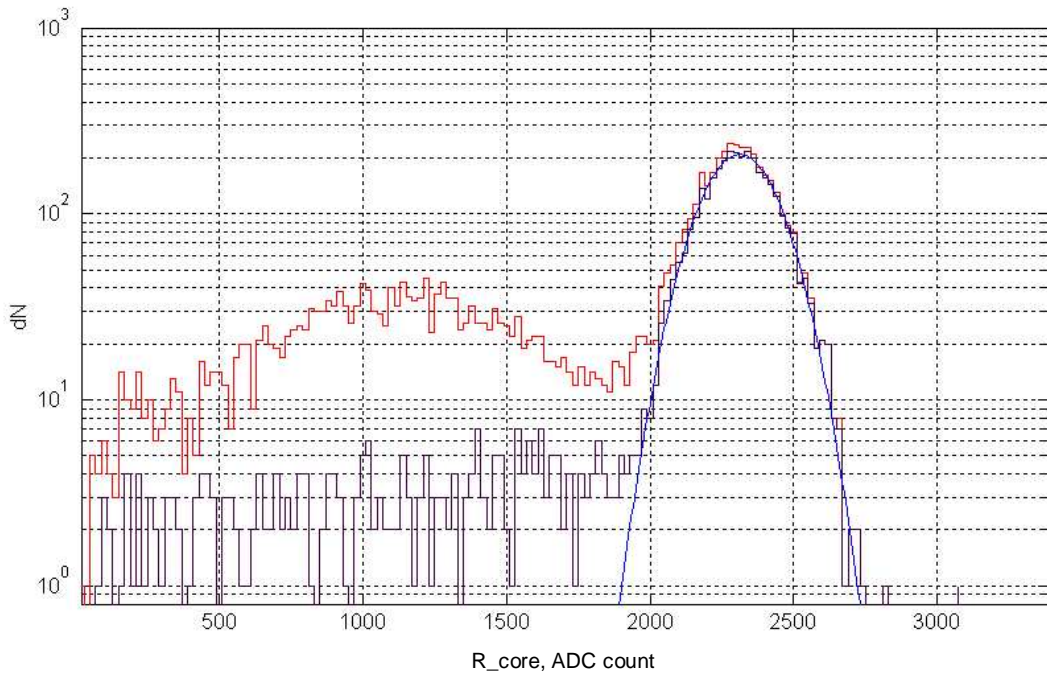


Fig.7. The distributions of $R_{core(8cm)}$:
— data, — data(cut), — Gauss,
cut: $0.9 < R_{core(4cm)}/R_{total} < 1.05$

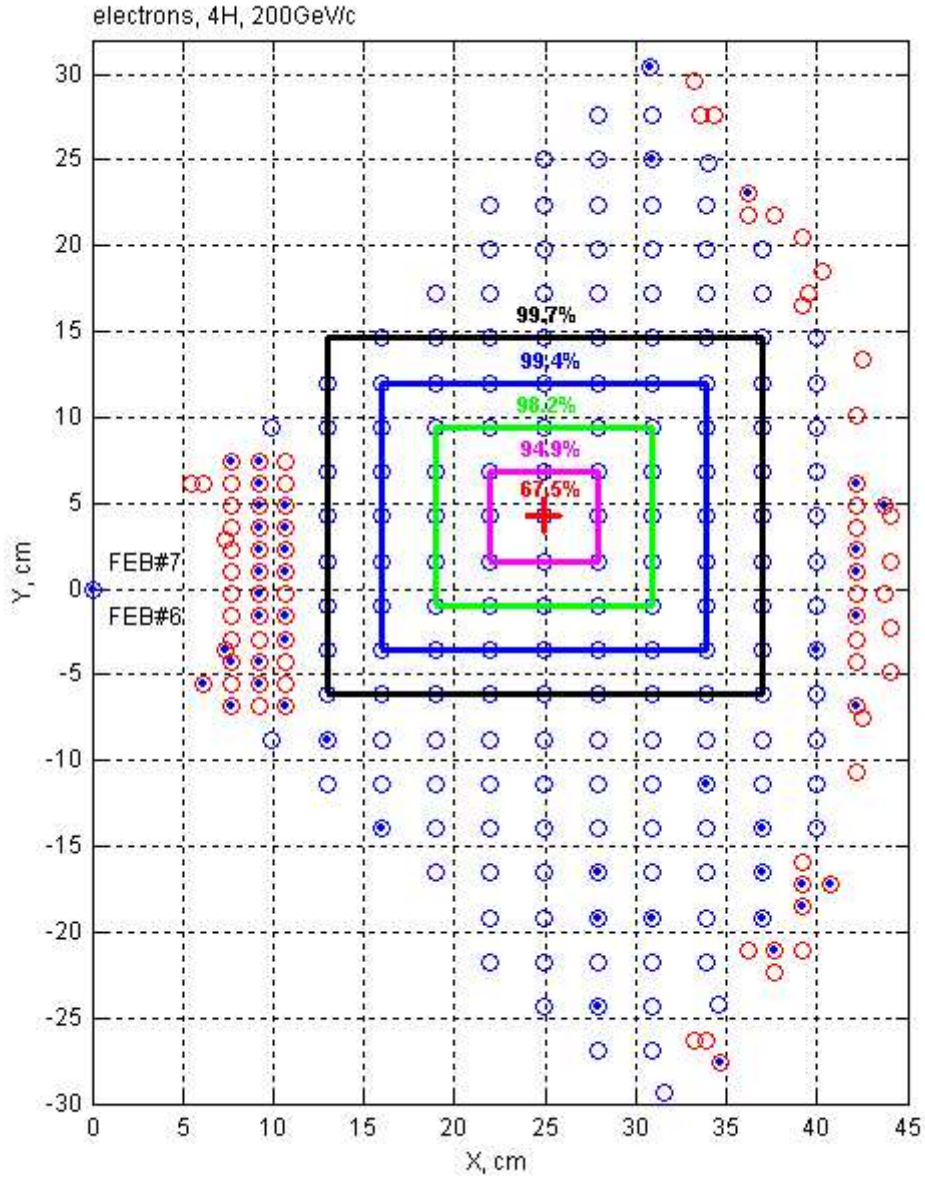


Fig.8. FCAL1 map, electrons, 4H, 200GeV/c:

- + - beam position
- o - cell centers,
- o - cells with 4 tubes,
- . - cells with “negative” energy R,
- - energy deposited inside a contour,

Min(R)=-0.15 ADC count. Total “negative” R=-1.8 ADC count (-0.08%R).

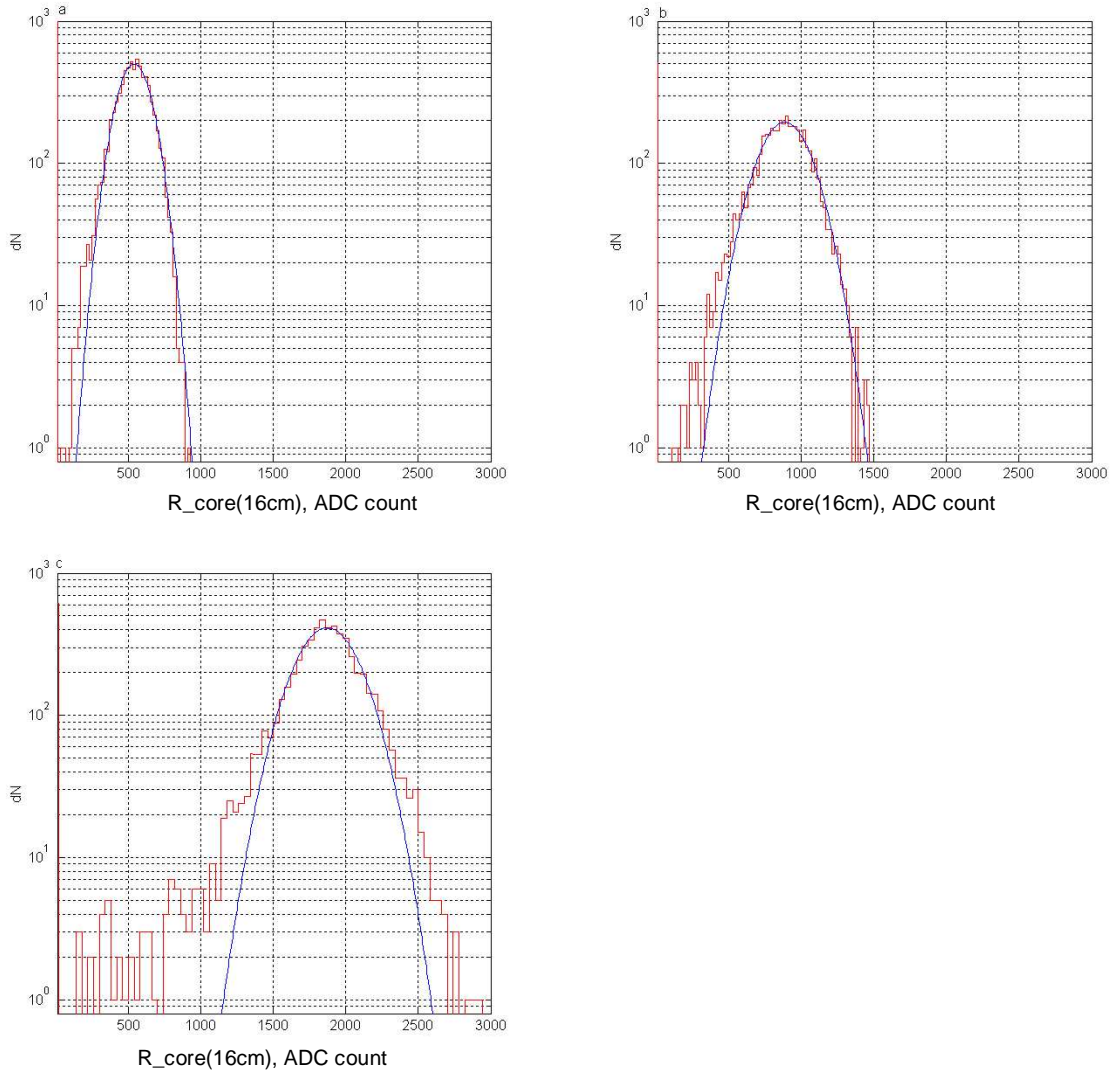


Fig.8. Distribution of $R_{core}(16cm)$, pions, 4H, a – 60GeV/c, b – 100GeV/c, c – 200GeV/c

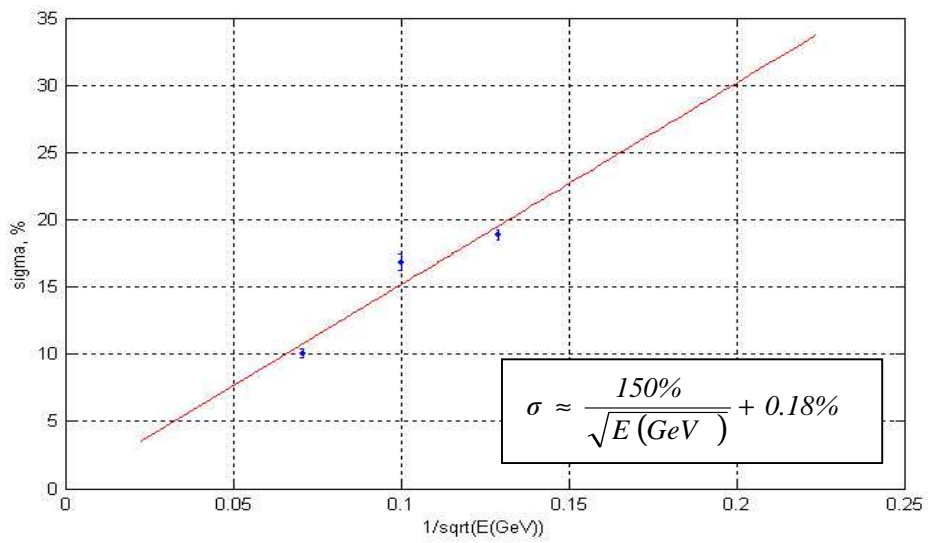


Fig.9. $\sigma(R_{core}(16cm))$ vs. $1/\sqrt{E}$ for pions, 4H, with the electronic channel noise quadratically subtracted

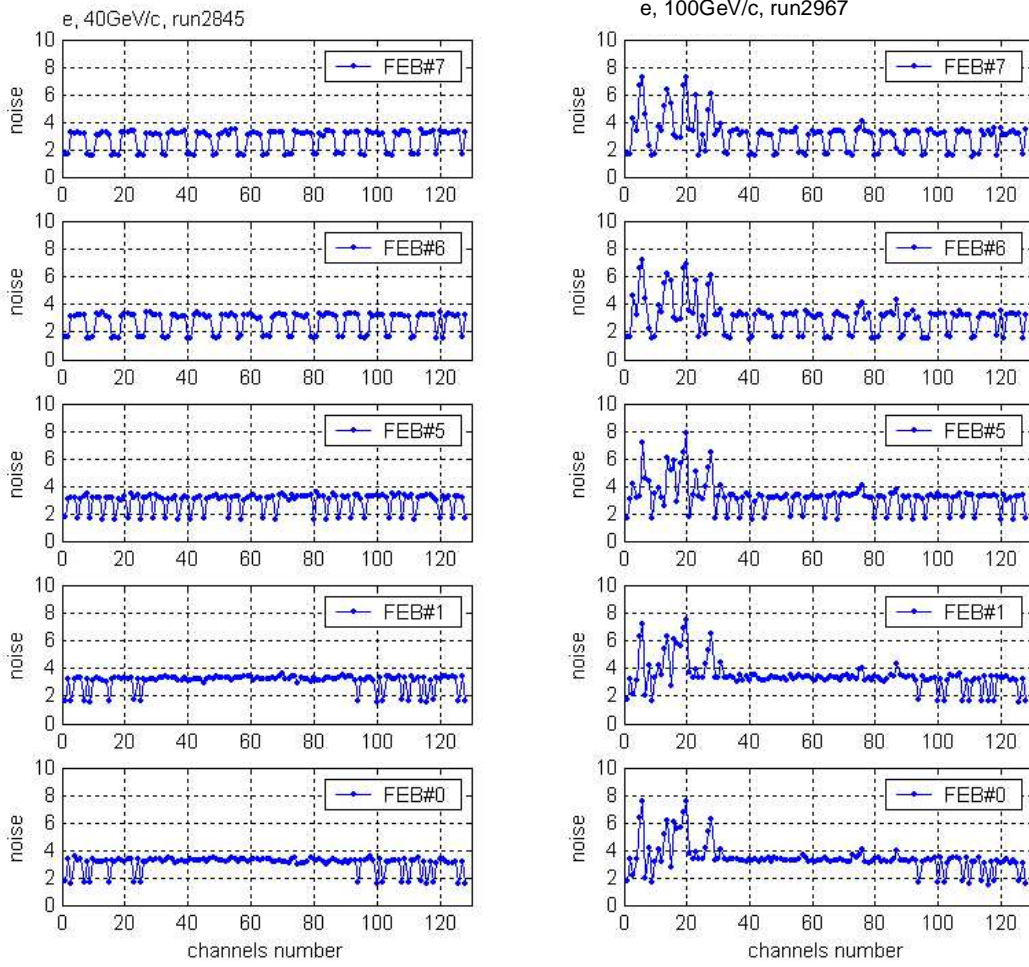
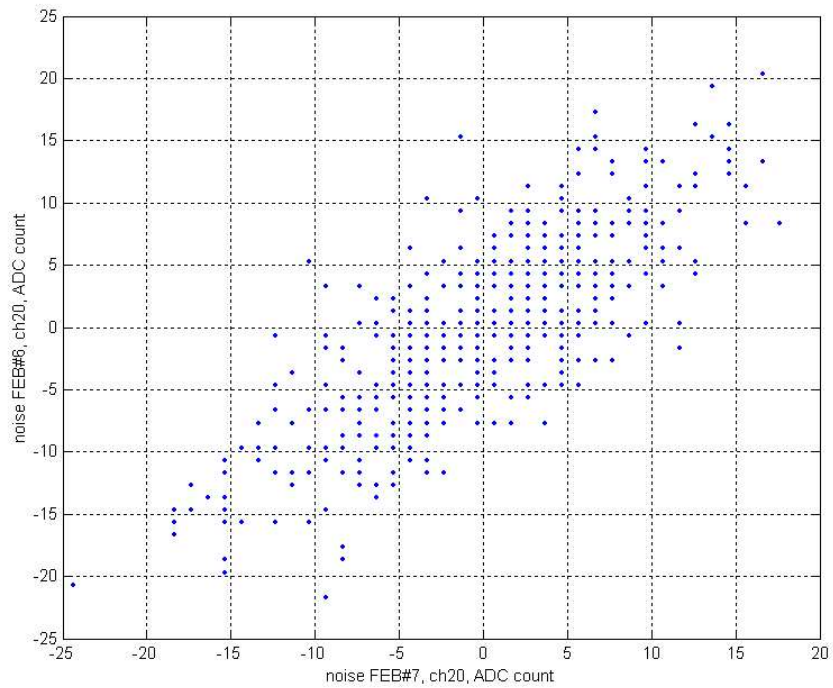


Fig.10. Channel noise in different FEBs, in ADC counts



Puc.11. An example of a correlated noise in FEB6 and FEB7 (channel 20), π , 4H, 100GeV/c